Revue des Composites et des Matériaux Avancés-Journal of Composite and Advanced Materials
Vol. 35, No. 6, December, 2025, pp. 1025-1031
Journal homepage: http://iieta.org/journals/rcma

Improving the Properties of the Gas Sensor Prepared from SnS, SnS:CNTs Films for the Detection of Environmental Pollutants

Abeer S. Alfayhan[1*], Ali J. Khalaf[2], Safa A. Jabbar[3], Nahida B. Hasan[1]

[1] Department of Physics, College of Science, University of Babylon, Babylon 51002, Iraq
[2] Radiology Techniques Department, College of Medical Technology, The Islamic University, Najaf 54001, Iraq
[3] Department of Physics, College of Education for Pure Science, University of Babylon, Babylon 51002, Iraq

Corresponding Author Email: s.ahmed@uobabylon.edu.iq

Copyright: ©2025 The authors. This article is published by IIETA and is licensed under the CC BY 4.0 license (http://creativecommons.org/licenses/by/4.0/).

https://doi.org/10.18280/rcma.350602

Received: 6 November 2025
Revised: 9 December 2025
Accepted: 26 December 2025
Available online: 31 December 2025

Keywords:
environmental pollutants, gas sensor, sensitivity, response time, recovery time, NO_2

ABSTRACT

We prepared thin films of SnS and SnS:CNTs with different weights using a drop casting method. The surface morphology of thin films was examined using the atomic force microscope technique (AFM). The results showed a sense of homogeneity. The roughness average, the root mean square (RMS) value, and the average grain size increased as the weight ratios increased. Optical properties were characterized using a UV-Visible Spectrophotometer (2700) across a spectrum ranging from 300 to 1100 nm. An increment in absorbance was noted with the rise, whereas the direct bandgap exhibited a decrease from 3.5 to 3.1 eV. The film's exceptional potential for sensor applications. The samples are tested for gas NO_2 in a temperature range of 150-250℃. Sensitivity, response time, recovery time, and selectivity of samples are studied. The results showed that the SnS and SnS:CNTs thin films produced are good candidates to be used as sensors. NO_2 gas sensors were tested on the films. Films' gas sensitivity decreases with temperature. The sensor's sensitivity has decreased due to the films' fluctuating working temperature. The reaction time of the gas sensor increased gradually, but recovery time decreased at operational temperature.

1. INTRODUCTION

Nitrogen dioxide (NO_2) is a highly toxic and reactive gas that plays a significant role in air pollution and is associated with respiratory problems. Its detection is crucial for environmental monitoring, industrial safety, and public health. Recently, SnS (semiconductor nanostructure) and SnS:CNTs (semiconductor nanostructure: carbon nanotube) membranes have emerged as highly effective materials for NO_2 gas sensing. These materials offer outstanding sensitivity, selectivity, and stability, making them suitable for a wide range of applications in NO_2 detection [1]. The detection of NO_2 gas using SnS and SnS:CNTs membranes primarily relies on the chemiresistive sensing mechanism. When NO_2 comes into contact with the SNS or SnS:CNTs material, it usually reacts in a way that causes electrons to move between the gas molecules and the surface of the semiconductor [2]. The material's electrical resistance or conductivity changes as a result of this transfer, allowing for measurement and correlation with the gas concentration. NO_2 is an oxidizing gas, which means it can accept electrons from the semiconductor material, leading to a decrease in the electron concentration in the SNS surface. As a result, the material's resistance increases [3, 4]. This increase in resistance is directly related to the concentration of NO_2 in the surrounding environment. In SnS:CNTs composites, the CNTs facilitate faster electron transport through the material, resulting in a more rapid response to changes in NO_2 concentration. The high conductivity of the CNTs also helps to amplify the signal, making the sensor more sensitive to low concentrations of NO_2 SnS and SnS:CNTs membranes offer exceptional performance for NO_2 gas detection due to their high sensitivity, selectivity, fast response time, and long-term stability [5]. Adding carbon nanotubes to SNS materials boosts how well electrons move and makes the sensor work better, which makes these materials perfect for many uses in the environment, industry, and health. As research and development in this field continue to progress, SnS and SnS:CNTs-based NO_2 sensors are expected to play a crucial role in ensuring cleaner air and safer environments [6]. Adding carbon nanotubes to SnS improves electrical conductivity, mechanical strength, and charge transport, enhancing performance in batteries and sensors [7].

2. EXPERIMENTAL

Sulfide of tin (SnS) This substance comes in the form of a brown powder that has a strong smell when mixed with water most common stable phase at room temperature: Orthorhombic Pbnm (similar to α-SnS, Herzenbergite). Carbon nanotubes, or CNTs, are Single-walled carbon nanotubes (SWCNTs) with a length of 2–10 μm and a

thickness of 1–2 nm were bought from a reliable source and used without any further cleaning. Following the doping method is a simple, fast, and low-cost technique to deposit a thin layer of nanoparticles, nanotubes, onto a flat substrate. Prepare. The material SnS, SnS:CNTs, is dispersed in a volatile liquid (solvent) like water This creates a homogeneous suspension or and Clean the Substrate: A target surface (substrate) glass slide is thoroughly cleaned to ensure the liquid spreads evenly. Deposit the Drops: Using a pipette 10-100 µL) of the dispersion is dropped onto the substrate's surface. The drops spread out, covering a defined area Dry and Form a Film The solvent is allowed to evaporate at room temperature o. As it dries, the solid material is left behind on the substrate, forming a non-uniform, thin particulate film or coating. AFM was used to look at the thin films that were made. This high-resolution microscope operates at normal atmospheric pressure, using a silicon nitride cantilever with a sharp tip to scan thin film surfaces. Its advanced imaging clearly reveals differences caused by preparation methods and impurities. UV-visible spectrometers, Absorptance, transmittance, and Eg were used to test the optical properties of the thin films that were made. Measurements for Gas Sensing How to Make Sensors: We used a drop-casting method to place a thin film of the SnS:CNTs composite on a ceramic base, spacing the sensors evenly. Controlling the film thickness made sure that the sensitivity stayed the same. Gas Exposure: The sensor was put in a controlled setting and exposed to different concentrations of target gases (NO_2) at 5 ppm, 10 ppm, and 20 ppm. Tests of Sensing: We checked the gas sensing characteristics for response time, recovery time, and sensitivity. We tracked the change in the sensor's resistance when exposed to target gases to determine the reaction. Environmental Monitoring: To test the sensor's ability to find real-world pollutants in the environment. the mathematical formula used to calculate Sensitivity (S%).

$$\text{Sensitivity(s)} = \Delta R/Rg = |Rg - Ra/Rg| \times 100\%$$

where,

Ra: is resistance of the film sensor in air presence.

Rg: is resistance of the film sensor in a gas presence.

3. RESULT

Atomic Force Microscopy (AFM) is a powerful imaging technique used to characterize surfaces at the nanoscale. It works by scanning a sharp tip (probe) over the surface, measuring the interactions between the tip and the sample surface [7]. AFM provides detailed topographical, mechanical, and electrical properties of the sample surface. This technique is essential for studying materials with a high degree of surface sensitivity. AFM plays a key role in characterizing the surface of SnS and SnS:CNTs at the atomic scale [8]. Figure 1(a) shows an Atomic Force Microscopy (AFM) scan of SnS (Tin Sulfide) in two directions, showing the surface topography with a scale for changing height. In the X-direction (horizontal), the scan goes across a horizontal area (0.31 µm), which shows how the material's surface traits, such as peaks and valleys, change as you move across it. The changes in height from 0 to 40.8 nm show any flaws or rough spots along the scan direction. This is important for figuring out the material's surface structure and possible electronic or optical properties and Y-direction (up and down): This scan also goes up and down 0.31 µm and shows the same surface features going up and down [9, 10]. Changes in the vertical direction show the overall surface topology of the SnS compound. This could show grain boundaries, surface defects, or other structural irregularities that are useful for uses in electronics or optoelectronics. Figure 1(b) represents the SnS compound represented in three directions. X-axis (horizontal): This represents one dimension of the surface, with the scale provided as 0.31 µm. The variations along the X-axis show the distribution of surface features like hills, valleys, and flat areas, Y-axis (vertical): Similar to the X-axis, the Y-axis is also scaled at 0.31 µm. The variations here provide information about how the material surface changes when observed from different angles, and the roughness pattern is likely replicated across this dimension too and Z-axis (height): This axis represents the height of surface features (as shown by the color scale, which ranges from 0 to 41 nm). The height variations give insight into the roughness and texture of the SnS surface.

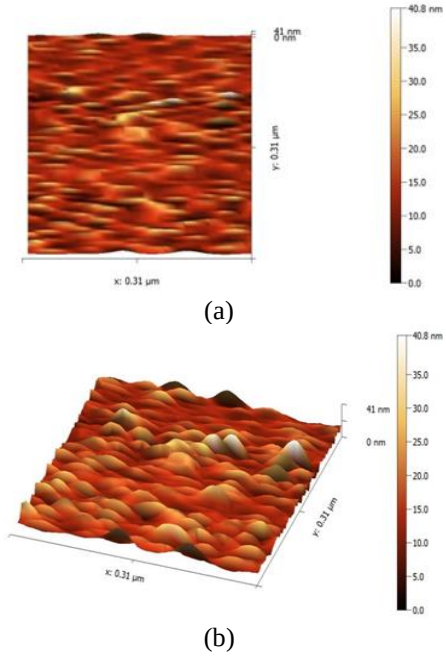

Figure 1. (a) 2-D (b) 3-D images of SnS pure thin films at 0.1 g

In 2D (Figure 2), the surface features displayed in the image are characterized by small, uneven, and rough patterns, which may indicate the composite's nanostructure properties. The surface exhibits significant roughness, with varying heights in the range of nanometers (up to 34.5 nm) (Figure 2). The material appears to have a complex surface with several small regions of varying heights, potentially corresponding to the SnS and CNTs phases or regions of the composite material [11]. The color scale on the side suggests that the image was taken with height information, with the darker colors corresponding to lower regions and the lighter colors representing higher regions. This topographical view could help us understand the surface shape of the SnS:CNTs composite, showing how the addition of CNTs affects the material's texture or structure. This type of analysis could be important for applications in electronics, energy storage, or catalysis [12]. The surface plot displays variations in surface height, indicating how the material's properties (such as roughness or morphology) change across a defined area. The

color scale on the right shows the height values in nanometers, ranging from 0 to 31.2 nm. The x and y axes represent the spatial dimensions, each scaled to 0.31 µm, giving a visual of the surface structure at a very fine scale, which is critical for analyzing the material's characteristics at the nanoscale.

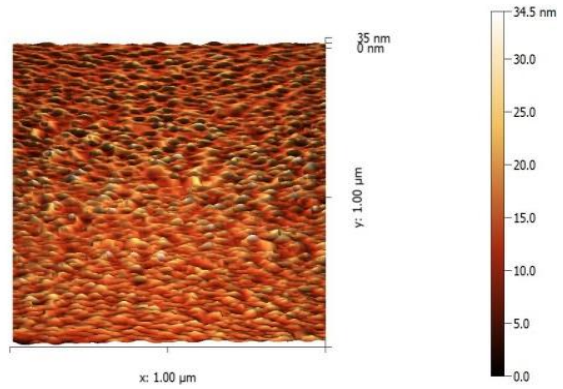

(a)

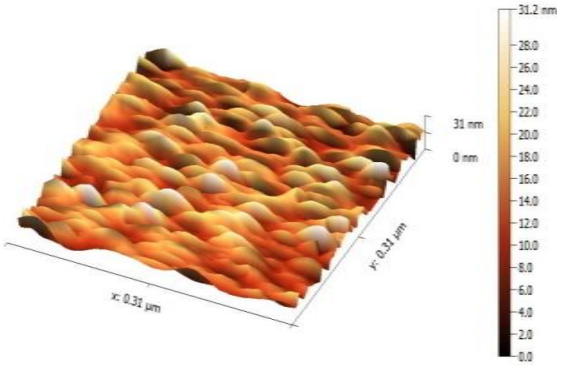

(b)

Figure 2. (a) 2-D (b) 3-D images of $SnS_{0.09gm:}$ $CNTs_{0.01gm}$ thin films

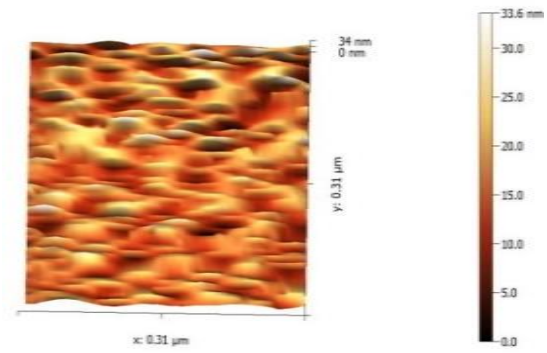

(a)

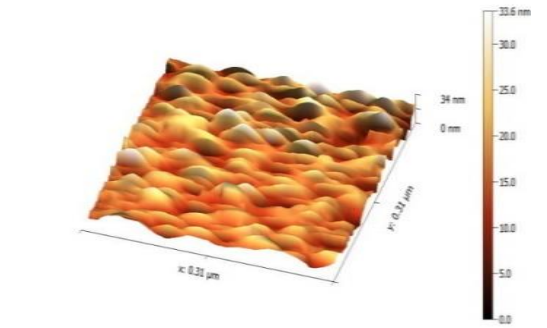

(b)

Figure 3. (a) 2-D (b) 3-D images of $SnS_{0.08gm:}$ $CNTs_{0.02gm}$ thin films

In 2D (Figure 3(a)), the surface is characterized by uneven, wave-like structures, indicating variations in height across the sample. This can represent the morphology of the SnS (tin sulfide) doped with carbon nanotubes (CNTs), showing how the dopant affects the surface topology. The height scale ranges from 0 to 34 nm, suggesting that the surface has features on the nanometer scale. This scale could be related to the crystallinity or roughness of the material. The color map next to the image indicates a gradient of heights, with darker shades corresponding to lower points and lighter shades to higher ones. In 3D (Figure 3(b)), the image appears 3D surface plot of the SnS:CNTs (tin sulfide/carbon nanotube) complex, with the specific doping of SnS at 0.03. The topography displayed in the plot shows nanoscale variations in height (ranging from 0 nm to 34 nm). These variations likely represent the distribution of atomic or molecular structures on the surface of the material, which could be related to the incorporation of carbon nanotubes into the SnS matrix. The color scale on the side correlates to the height variations in the plot, indicating areas of higher or lower surface features. The "x" and "y" axes indicate the dimensions of the surface area at the nanoscale (0.31 µm), showing the area covered in the measurement.

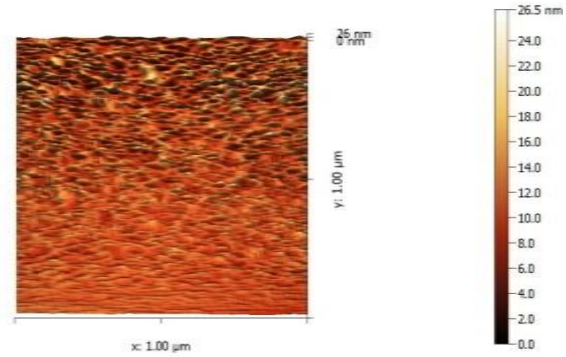

(a)

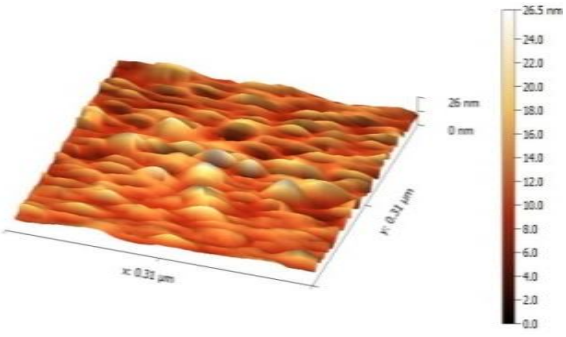

(b)

Figure 4. (a) 2-D (b) 3-D images of $SnS_{0.07gm:}$ $CNTs_{0.02gm}$ thin films

In 2D (Figure 4(a)), the surface displays varying heights, with a height range from 0 to 26.5 nm, indicating microstructural variations within the composite. X and Y Axes: Both axes represent the scale of 1.00 µm, giving an idea of the material's fine surface details over a microscopic area . The doping concentration of SnS and CNTs may have influenced the surface roughness, which is visible in the structure and variations across the surface. The image reflects the intricate surface texture of the composite at the nanoscale, which is important in studying its properties such as electrical conductivity, mechanical strength, or interaction with other

materials. In 3D (Figure 4(b)), the image showcases the roughness and undulating structure of the composite material's surface. The height variation ranges from 0 to 26 nm, indicating the microstructural features of the SnS:CNT composite. The surface exhibits wavy, smooth hills and valleys that may result from the incorporation of CNTs into the SnS matrix. This morphology could influence the material's overall properties, such as conductivity or mechanical strength. Fine Scale: The dimensions of the image (0.31 μm by 0.31 μm) represent a very fine scale, useful for studying the nanoscale interactions between the SnS and CNTs components. Overall, this 3D image gives insight into the material's surface morphology and how the doping and CNTs density influence the structural characteristics. We notice that increased surface roughness (from added CNTs) creates more active sites for gas adsorption, enhancing NO_2 absorption on the SnS surface.

3.1 Optical properties

The optical properties of SnS:CNTs films deposited on a glass substrate have been determined using the UV-VIS-IR transmittance spectrum in the range of (300-1100) nm. he optical properties of materials provide critical insights into their interaction with light, influencing their potential applications in electronics, photovoltaics, and optoelectronic devices. For the SnS:CNTs composite, these properties were measured to evaluate how the inclusion of carbon nanotubes (CNTs) affects the overall performance and functionality of the tin sulfide (SnS) matrix.

3.2 Absorbance spectrum

Figure 5 shows the relationship between the absorbance and wavelength of SnS and SnS:CNTs films. This property quantifies the amount of light absorbed by the material when exposed to electromagnetic radiation, typically in the ultraviolet-visible (UV-Vis) spectrum. Absorbance is directly related to the electronic transitions within the material and is crucial for understanding its ability to harness light, especially in photovoltaic applications. The increase in absorbance of SnS (tin sulphide) when doped with different proportions of CNTs (carbon nanotubes) can be explained by a combination of optical, structural, and electronic effects introduced by the CNTs. Enhanced light absorption due to CNT intrinsic properties Carbon nanotubes has a broad optical absorption spectrum, covering the visible and near-infrared regions. When CNTs are added to SnS, their own light absorption contributes to the total absorbance of the composite, effectively adding extra absorbing centres. Electronic structure modification (band gap tailoring) Doping SnS with CNTs can cause changes in its band structure due to interaction between the π-electrons in CNTs and the electronic states of SnS. This can lead to band gap narrowing, which allows SnS to absorb photons of lower energy (longer wavelengths), thereby increasing the measured absorbance [8].

Transmittance Spectrum-22

Figure 6 shows the relationship between transmittance and wavelength of SnS and SnS:CNTs. The interface between the SnS and CNTs might lead to the scattering of charge carriers, disrupting the coherent alignment of the magnetic dipoles in the SnS. Such changes can reduce the contribution of SnS to the overall magnetic permeability. Changes in electron mobility: CNTs can alter the charge transport properties within the SnS matrix. This may lead to changes in the electronic structure, which could affect the magnetic behaviour, particularly the alignment of magnetic moments in the material. Disruption of Crystal Lattice, Introducing CNTs into the SnS crystal lattice could disturb its atomic or molecular arrangement, leading to a reduction in the material's ability to sustain its intrinsic magnetic properties. In summary, CNT doping alters the magnetic behaviour of SnS by diluting its magnetic components, introducing scattering centres, and disrupting its overall structure, all of which lead to a decrease in magnetic permeability [10].

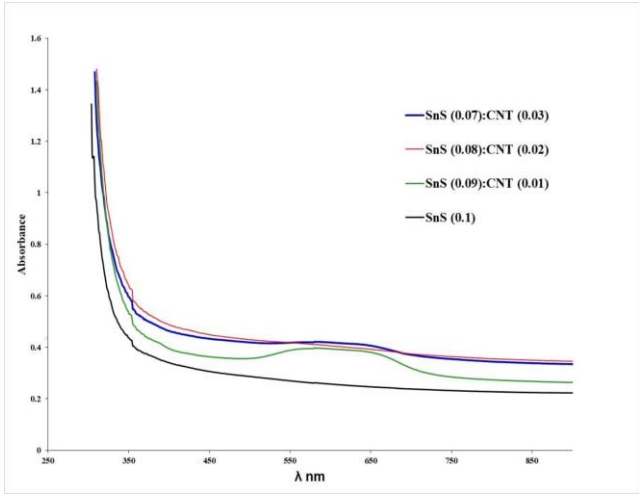

Figure 5. Absorbance spectrum as a function of wavelength for SnS and SnS:CNTs thin films at with different doped

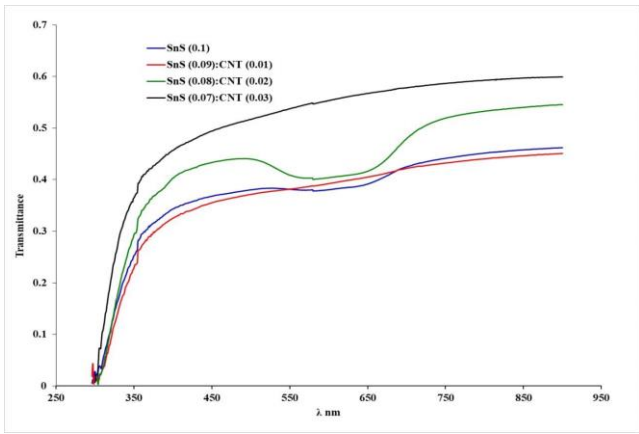

Figure 6. Transmittance spectrum as a function of wavelength as a function of wavelength for SnS and SnS:CNTs thin films at with different doped

3.3 Optical energy gap

From Figure 7, the optical energy gap of SnS and CNTs films deposited on glass substrates. Adding doped carbon nanotubes (CNTs) to SnS lowers its energy gap. This is mostly because the two materials interact electronically and change their band structures. It is a p-type semiconductor and its band gap is between 1.1 and 1.3 eV, based on the crystal phase and thickness. Strain, flaws, and the way it interacts with other materials can change its band structure. Doping CNTs has an effect Nanotubes of carbon can be metal or semiconducting. Adding N, B, or other atoms to them changes their Fermi level

and DOS, which stands for "density of states." Most of the time, doped CNTs have extra electronic states close to the Fermi level that can connect with the bands of the semiconductor. Reduced energy bandgap (due to CNT incorporation) improves the electronic response by facilitating easier electron transfer between SnS and NO_2 molecules.

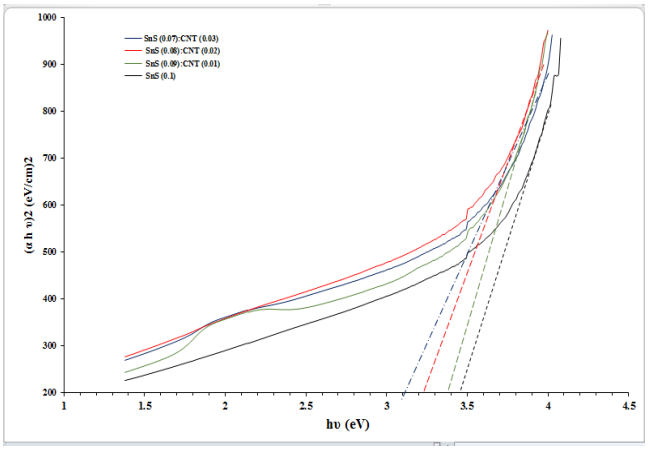

Figure 7. The optical energy gap for the allowable direct transition for SnS and SnS:CNTs thin films at with different doped

4. GAS SENSING MEASUREMENT FOR SNS AND SNS:CNTS THIN FILMS

4.1 The determination of the operational temperature of the sensor

Depending on the specific sensor used, the concentration of the gases, and the environmental conditions, the optimal operating temperature for a sensor detecting NO_2 gases can vary. Figure 8 shows the relationship between sensitivity and operating time for SnS, the efficient electron transfer from p-SnS to NO_2, increasing hole concentration and conductivity. The sensor's response (sensitivity) is calculated based on this change in conductivity (or resistance). Therefore, as more NO_2 adsorbs, the conductivity increases dramatically, leading to a rising sensitivity. When SnS is exposed to NO_3, the gas molecules adsorb onto the surface of the SnS crystals. NO_2 is a strong oxidizing gas. Electron Extraction: Upon adsorption, NO_2 molecules extract electrons from the SnS material. The reaction can be represented as:

$$NO_2\ (gas) + e^- \rightarrow NO_2^-\ (adsorbed)$$

In the SnS/CNT hybrid (Figures 9 and 10), the highly conductive CNTs create a fast path for electrons. Since most of the electrical current flows through the CNT network, the change in SnS's conductivity upon gas exposure has a minimal effect on the overall resistance of the material. The signal from the sensitive SnS is essentially "shorted out" by the CNTs. Additionally, CNTs can block the active adsorption sites on the SnS surface, further reducing its interaction with gas molecules. In Figure 11 Increased doping with CNTs in SnS films leads to higher sensitivity primarily because the CNTs create a more extensive conductive network. This network provides more pathways for electron transport, resulting in a larger change in electrical conductivity when the film is exposed to a target gas, which is the fundamental principle of chemiresistive gas sensors. Table 1 shows the relationship between sensitivity and temperature [11, 12]. We do not observe an increase in surface roughness and increased absorbance, while the energy gap value decreases Together, these factors significantly boost the sensor's sensitivity and response to NO_2, as more gas molecules are effectively adsorbed and detected through measurable changes in electrical resistance [13].

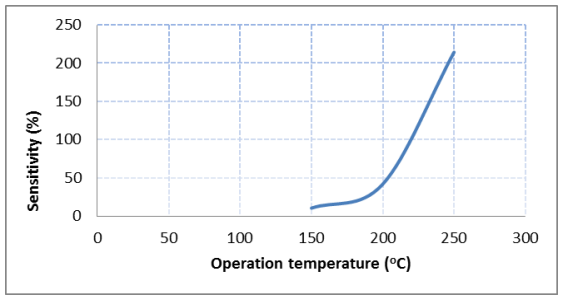

Figure 8. The relationship between sensitivity and operating time for SnS thin film

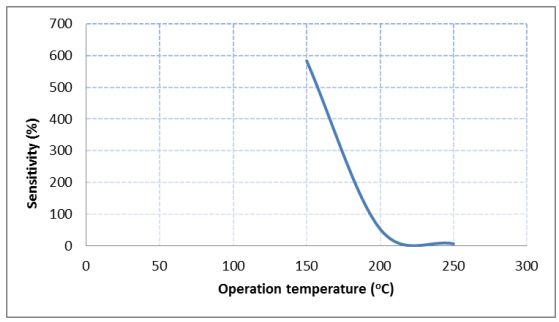

Figure 9. The relationship between sensitivity and operating time for $SnS_{0.09gm}$: $CNTs_{0.01gm}$ thin film

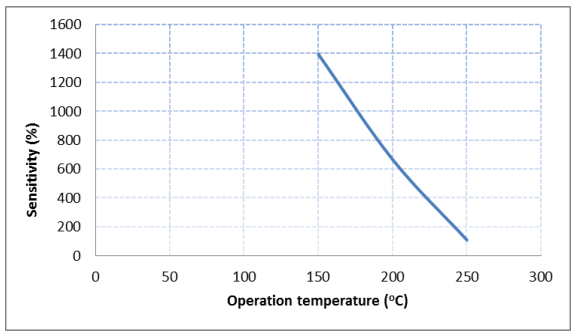

Figure 10. The relationship between sensitivity and operating time for SnS $_{0.08gm}$: CNTs $_{0.02gm}$ thin film

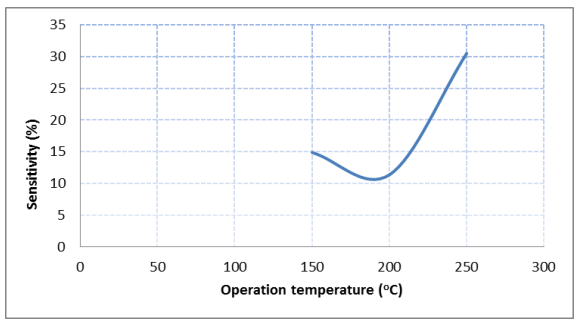

Figure 11. The relationship between sensitivity and operating time for SnS $_{0.07gm}$: CNTs $_{0.03gm}$ thin film

Table 1. The relationship between sensitivity and temperature

	Sample	Sensitivity (%)	Operating Time
1	SnS $_{0.1gm}$	10.47234307 41.78262505 214.4 583.9979808	150 200 250
2	SnS $_{0.09gm}$: CNTs $_{0.01gm}$	52.79232112 6.25 1395.711835	
3	SnS $_{0.08gm}$: CNTs $_{0.02gm}$	666.3967611 109.0443686 14.88340192	
4	SnS $_{0.07gm}$: CNTs $_{0.03gm}$	11.35678392 30.51470588	

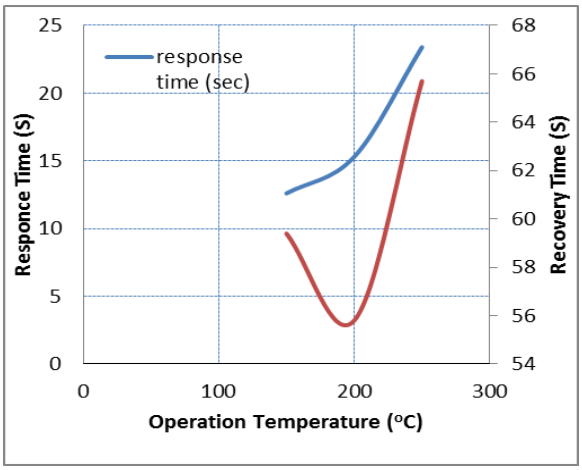

Figure 12. The relationship between response time (sec) and recover time (sec) for SnS thin film

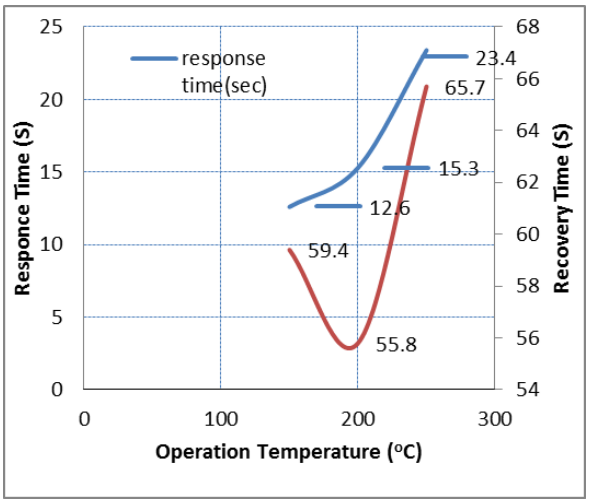

Figure 13. The relationship between response time (sec) and recover time (sec) for SnS $_{0.09gm}$: CNTs $_{0.01gm}$ thin film

4.2 Response time and recovery time

The time interval during which the resistance of the sensor material reaches a fixed percentage (usually 90%) of its final value when exposed to full-scale gas concentration [14, 15]. A short response time is highly desirable in applications such as detecting flammable or combustible gases to prevent fires [16]. In Figure 12, we notice that the operating time and recording time have increased for Sn The import and registration time increase in SnS during gas sensor fabrication because the process involves more complex data, additional calibration parameters, and extra verification steps required for gas sensor accuracy (Figures 13-15). The addition of Carbon Nanotubes (CNTs) to Tin Sulfide (SnS) creates a composite material with improved but more complex electrical properties, leading to the observed changes in response and recovery times [17]. The highly conductive CNTs form a network within the semiconducting SnS matrix. This provides fast pathways for electrons to travel, allowing the sensor to register a change (e.g., gas adsorption) much more quickly [18, 19]. In short: CNTs act as electronic highways for fast response, but their interfaces act as traffic traps that slow down the recovery [20, 21].

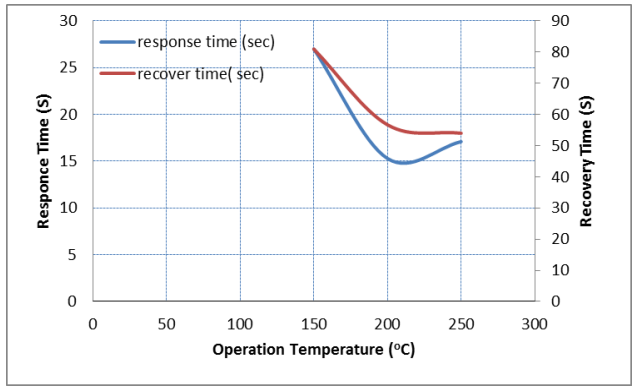

Figure 14. The relationship between response time (sec) and recovery time (sec) for SnS $_{0.08gm}$: CNTs $_{0.02gm}$ film

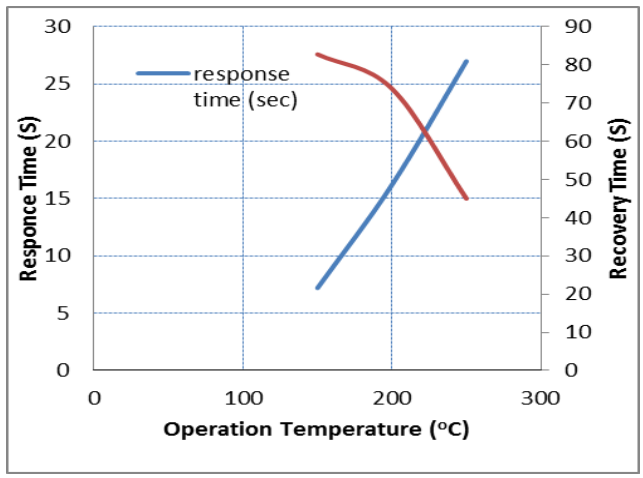

Figure 15. The relationship between response time (sec) and recover time (sec) for SnS $_{0.07gm}$: CNTs $_{0.03gm}$ thin film

5. CONCLUSIONS

Film Properties: Homogeneous SnS and SnS:CNTs thin films were successfully fabricated. Their surface roughness and grain size increased with higher weight ratios. Optical Properties: The films showed increased light absorption and a decrease in the direct bandgap from 3.5 eV to 3.1 eV. Gas Sensing Performance: The films demonstrated good potential as NO_2 gas sensors. However, sensitivity decreased with increasing operating temperature (150–250°C), while response time increased and recovery time decreased. Overall

Conclusion: SnS and SnS:CNTs thin films are promising candidates for gas sensor applications, despite a trade-off between sensitivity and operating temperature.

ACKNOWLEDGMENT

The authors would like to acknowledge the assistance offered by the Department of Physics in the College of Science, University of Babylon /Iraq.

REFERENCES

[1] Mittal, M., Kumar, A. (2014). Carbon nanotube (CNT) gas sensors for emissions from fossil fuel burning. Sensors and Actuators B: Chemical, 203: 349-362. https://doi.org/10.1016/j.snb.2014.05.080

[2] Gadtya, A.S., Mahaling, R.N., Rout, L., Moharana, S. (2024). Carbon nanotube-based polymer nanocomposites for aerospace applications. In Carbon Nanotube-Polymer Nanocomposite, pp. 435-459. https://doi.org/10.1007/978-981-97-6329-0_17

[3] Sharma, S., Meena, P.K., Nayak, C., Burande, C.G., Shrivastava, A., Chaturvedi, R. (2025). Enhancing biogas production from lignocellulosic biomass: Challenges, innovations, and sustainability pathways. Environmental Progress & Sustainable Energy, e70251. https://doi.org/10.1002/ep.70251

[4] Alfayhan, A.S., Hasan, N.B. (2025). Gas sensor for NH3 and NO2 gases: Analyzing optical dielectric constants in real and imaginary domains. Journal of Interdisciplinary Mathematics, 28(1): 185-195. https://doi.org/10.47974/JIM-1848

[5] Sadaqat, A., Ali, G., Hassan, M.U., Iftikhar, F.J., Abbas, S. (2023). Ni3S4/SnS/graphene oxide/carbon nanotube composites as anodes for Na-ion batteries. ACS Applied Nano Materials, 6(3): 1996-2008. https://doi.org/10.1021/acsanm.2c05002

[6] Khalaf, A.J., Alfayhan, A.S., AL-Shareafi, M.A. (2022). Synthesis gas sensor from CuFe2O3: Cu films by spin coating. WSEAS Transactions on Applied and Theoretical Mechanics, 17: 94-101. https://doi.org/10.37394/232011.2022.17.13

[7] Alfayhan, A.S., Hasan, N.B. (2024). Influence of pulse laser deposition on the structural and optical properties of CZTS for sensor applications. Journal of Composite & Advanced Materials, 34(1): 95-102. https://doi.org/10.18280/rcma.340112

[8] Khaleel, A.Q., Kumar, A., Altalbawy, F.M.A., Sapaev, I.B., et al. (2025). Electronic, magneto-optic and band alignments of MnO2/AlN and MnO2/SiC topological vdW hetrostructures: A DFT study. Solid State Communications, 403: 115966. https://doi.org/10.1016/j.ssc.2025.115966

[9] Kadhim, S.M., Hamed, E.K., Abdullah, H.H., Dawood, Y.Z., Al-Hiti, A.S. (2024). Fabrication of nanocrystalline SnO2 films by Nd: YAG pulsed laser deposition method for gas sensor applications. Journal of Optics, 53: 4382-4391. https://doi.org/10.1007/s12596-024-01738-9

[10] Mahdi, M.A., Khadayeir, A.A., Kareem, Q.S., Shaheed, M.A. (2023). Effect of Zn doping in CuO optical and gas sensing properties. AIP Conference Proceedings, 2845(1): 070034. https://doi.org/10.1063/5.0157326

[11] Mohammed, H.R.A., Hasan, N.B., Shinen, M.H. (2025). Structural, morphological and optical properties of (NiO)1-x(Co3O4)x composite thin films prepared by chemical spray pyrolysis technique. Revue des Composites et des Matériaux Avancés-Journal of Composite and Advanced Materials, 35(2): 367-373. https://doi.org/10.18280/rcma.350218

[12] Khalaf, A.J., Alfayhan, A.S., Hussein, R.G.K. (2023). Synthesis gas sensor from compound Sb2O3: In2O3 by spin coating method. AIP Conference Proceedings, 2830(1): 070027. https://doi.org/10.1063/5.0157270

[13] Raman, A., Rachananjali, K., Khalaf, A.J., Manjunatha, R., et al. (2026). Two- and three-dimensional probe absorption measurements in diamond germanium-vacancy color centers. Applied Optics, 65: 373-373. https://doi.org/10.1364/AO.584002

[14] Ibrahim Mohammad, S., Hemza, S., Vasudevan, A., Sanaan Jabbar, H., Sapaev, I.B., Sharma, M.K., Nikpendar, A. (2025). Optimizing lithium–sulfur batteries by tailoring heterogeneous pore structures and surface chemistry in porous sulfur–carbon nanocomposites. Composite Interfaces. https://doi.org/10.1080/09276440.2025.2593694

[15] Hjiri, M., Dhahri, R., Barakat, F.M., Neri, G. (2025). Sb2O3, Sb2O5, and Sb-doped based resistive gas sensors: A review. Brazilian Journal of Physics, 55: 217. https://doi.org/10.1007/s13538-025-01850-6

[16] Schroeder, V., Savagatrup, S., He, M., Lin, S., Swager, T.M. (2019). Carbon nanotube chemical sensors. Chemical Reviews, 119(1): 599-663. https://doi.org/10.1021/acs.chemrev.8b00340

[17] Luo, S.X.L., Swager, T.M. (2023). Chemiresistive sensing with functionalized carbon nanotubes. Nature Reviews Methods Primers, 3: 73. https://doi.org/10.1038/s43586-023-00255-6

[18] Luo, K., Peng, H.R., Zhang, B., Chen, L.M., Zhang, P.P., Peng, Z.J., Fu, X.L. (2024). Advances in carbon nanotube-based gas sensors: Exploring the path to the future. Coordination Chemistry Reviews, 518: 216049. https://doi.org/10.1016/j.ccr.2024.216049

[19] Mohammad, S.I., Vasudevan, A., Kareem, A.K., Arunkumar, D.T., Khalaf, A.J., et al. (2025). Chemically engineered TiO2 quantum dot-graphene nanocomposites for enhanced lithium-ion battery anode performance. Journal of Physics and Chemistry of Solids, 113396. https://doi.org/10.1016/j.jpcs.2025.113396

[20] Gautam, Y.K., Sharma, K., Tyagi, S., Ambedkar, A.K., Chaudhary, M., Pal Singh, B. (2021). Nanostructured metal oxide semiconductor-based sensors for greenhouse gas detection: Progress and challenges. Royal Society Open Science, 8(3): 201324. https://doi.org/10.1098/rsos.201324

[21] Al Mohamadi, H., Khalaf, A.J., Ali, R.H.M., Fayzullaev, N., Akkur, M., et al. (2026). NdCoO3 immobilized on Ag-modified reduced graphene oxide sheets for stable and high-efficiency hybrid electrochemical supercapacitor. Journal of Industrial and Engineering Chemistry. https://doi.org/10.1016/j.jiec.2026.01.008